Development of three electrode type micro-electrochemical reactor on anodized aluminum with photon rupture and electrochemistry

Masatoshi SAKAIRI[a,1], Masashi YAMADA[b], Tastuya KIKUCHI[a] and Hideaki TAKAHASHI[a,1]

[a]Graduate School of Engineering, Hokkaido University, Kita-13, Nishi-8, Kita-ku, Sapporo, 060-8628, Japan.

[b]Presently; MEMS Technology Division, Olympus Corporation, 6666 Inatomi, Tatsuno-machi, Kamiina-gun, Nagano, 399-0495, Japan.

Abstract

Photon rupture with a focused single pulse of pulsed YAG-laser irradiation was used to fabricate an aluminum electrochemical micro-reactor. Porous type anodic oxide film formed on aluminum specimens was irradiated in solutions with a pulsed Nd-YAG laser beam through a convex lens to fabricate micro channels, micro-electrode, and through holes (for reference electrode, solution inlet, and outlet). During irradiation, specimens were moved by a computer controlled XYZ stage. After irradiation, the surface of the micro-channel and through hole were again treated to form anodic oxide film and the surface of the micro-electrode was treated electrochemically to provide an Au layer. The calculated volume of the micro-reactor including micro-channel and through holes is about 1.5 µl. The cyclic voltammogram of the micro-electrochemical cell was measured in $K_3Fe(CN)_6$ / $K_4Fe(CN)_6$ with both static and flowing solution at different scanning rates. The anodic and cathodic peak currents were measured and the values depended on scanning rate and ion concentration when the solution was static. With the flowing solution, limiting currents were observed and the anodic limiting current was increased with the cubic root of the solution flow rate.

Key words: micro-reactor, anodizing, aluminum, LASER fabrication, deposition

*Corresponding author: Tel.: +81-11-706-7111; Fax.: +81-11-706-7881; e-mail: msakairi@eng.hokudai.ac.jp

1 ISE member

1. INTRODUCTION

Micro-reactor and micro miniaturized total analysis systems (μ-TAS) have been studied to investigate reduction in system size, waste solutions, and reagents, and to achieve high reaction rates [1-13]. This kind of equipment has been developed on silicon, glass, and organic sheets by mask processes, photo lithography and LIGA processes. Kamidate et al. developed micro-channels on glass by photo lithography and detected luminescence related bio-chemical reactions [4, 5]. Ueno et al. fabricated micro-electrochemical reactors on plastic by mold printing [6 - 9]. Organic electrochemical reactions [14, 15] and photo catalytic reactions [16] have also been studied using micro-electrochemical reactors.

Recently, oxide film stripping and surface patterning by photon rupture (focused pulsed Nd-YAG laser beam irradiation) has been reported [17]. The irradiation of a pulsed laser beam is able to strip the oxide film at extremely high rates (< 100 ns) without contamination from the film stripping tools. Chu et al. formed local nickel deposited layers by using a laser technique and electro-less plating [18 - 21]. Some of the present authors, Kikuchi et al. [22 - 24], reported that complete removal of selected parts of anodic oxide film, from aluminum substrate by laser irradiation followed by electro-deposition and dissolution of the aluminum substrate, enables the fabrication of well-ordered three-dimensional microstructures and printed circuit boards. Recently, this technique is successfully applied in the fabrication of micro-actuators [25] and micro-channels formed in an anodic oxide film [26].

Some of the present authors have developed two electrode type micro-electrochemical reactors on anodized aluminum by photon rupture and electrochemistry [27]. This micro-reactor made of aluminum has advantages, such as high electric and heat conductivity, and it is not fragile. However, the fabricated micro reactor is a two electrode system, and the meaning of the relationship between current and applied voltage is not clear. Therefore, there is an urgent need to develop a three electrode type micro-electrochemical reactor on anodized aluminum by this technique. The purpose of this study is to develop a three electrode type micro-electrochemical reactor by a combination of anodizing, laser irradiation and electroplating, and to determine its performance with actual electrochemical reactions the cyclic voltammograms of the developed micro-electrochemical reactor was measured.

2. EXPERIMENTAL

Specimen : Aluminum sheets, 99 mass %, 1 mm thick, were cut into 15 x 25 mm^2 specimens. The specimens were degreased in an ethanol ultrasonic bath, mechanically polished by SiC paper, and then electro-polished in a mixture of 70 mass % perchloric acid and acetic acid, volume ratio 1 : 4, at a constant cell voltage of 28 V at 286 K. After electro-polishing the specimens were rinsed in doubly distilled water and acetone.

Anodizing : Porous type anodic oxide films were formed by anodizing at 293 K in 0.22 $kmol/m^3$ oxalic acid solution with a constant current density, i_a = 100 A/m^2 for t_a = 3.6 ks at 298 K. The estimated film thickness is about 18 μm and the anodized area is 10mm x 15mm. After anodizing, specimens were dyed in 0.03 $kmol/m^3$ alizarin red-S

solution for 300 s at 323 K, and then sealed in boiling distilled water for 900 s.

Laser irradiation: After sealing, the specimens were immersed in solution and irradiated by a pulsed Nd - YAG laser (Sepctra Physics GCR - 130) beam through a lens and quartz window. The laser beam was the second harmonic wave, wave length 532 nm, wave duration 8 ns, and frequency 10 s^{-1}. The irradiation time, t_i, was varied between 0.18 s and 3.6 ks, and the laser power, P, between 5 mW to 50 mW. To fabricate micro-channels, through holes, and micro-chambers, the distance between the specimen and lens and the irradiated position were controlled by an XYZ stage. The surfaces of the irradiated area were observed by a confocal scanning laser microscope (CSLM).

Re-anodizing and Au electroplating: After forming micro-channels and through holes, the samples were anodized again in 0.22 $kmol/m^3$ oxialic acid solution, then micro-chambers, micro-electrodes of 2x2 mm were formed. After this gold was deposited on the micro chamber surfaces, electrochemically at a constant potential of E_p = - 0.7 V vs Ag/AgCl for 1.8 ks at 298 K, giving an estimated Au thickness of about 5 μm. Figure 1 is a schematic outline of the fabrication process of the micro-electrochemical cell.

Cyclic voltammetry (CV): The cross section of an electrochemical micro-reactor and electrochemical measurement unit is shown in Fig. 2. The CV of the micro-electrochemical cell was measured in $K_3Fe(CN)_6$ / $K_4Fe(CN)_6$ without flow (static) and with flowing solution at different scanning rates, at reagent concentrations of 2 mol/m^3, 20 mol/m^3 and 200 mol/m^3, in the reagent volume ratio 1:1. A coated Pt wire was used as the reference electrode. A micro-syringe pump, KD Scientific Inc.

KDS-200, was used to control the flow rate of solutions in the range 6.2 x 10^{-2} to 1 µl/s.

3. RESULTS

3.1 Fabrication of electrochemical micro-reactor

Figure 3 shows a top view of fabricated plates, I and II, with electrochemical micro-reactors, and Fig. 4 shows CSLM images of the different parts of the reactor. Figure 4 shows that the laser irradiated surface is smooth without cracks in the oxide film. These pictures shows that it is possible to make each of the elements of the micro-reactor with a combination of laser fabrication and electrochemistry, and without machining of the anodized aluminum plate. The through hole is about 350 µm in diameter, the dimensions of the micro-channel is about 250 µm wide and 2 mm long, and the depth is about 150 µm. The size of the micro-electrode is about 4 mm^2, the depth of the electrode is about 110 µm and the estimated Au coating thickness is about 5 µm.

After fabricating each element, nitrocellulose film coated Pt wire, 100 µm diameter, and fused silica tubes, 200 µm diameter, were mounted at each through hole. Figure 5 shows a) a schematic illustration and b) a top view of the assembled micro-reactor. Two plates are attached with silicon rubber and hold in place by clips. The calculated volume inside the reactor including the through hole and micro-channel is about 1.5 x 10^{-9} m^3 (1.5 µl).

3.2 Electrochemical performance at static conditions

Commonly used ferric and ferrous ion containing solutions were used to investigate the

electrochemical performance of the cell. Fig. 6 shows the CV obtained by the micro-reactor at static (non-flowing) conditions in [$K_3Fe(CN)_6$ + $K_4Fe(CN)_6$]. The concentration of the reagents was 200 mol/m^3 and 20 mol/m^3 (mixing ratio 1:1). The scanning rate was varied between 5 mVs^{-1} to 100 mVs^{-1}. There are anodic peaks at about 0.05V and the cathodic peaks can be seen at about - 0.05 V. The peak currents show very similar values at the same scanning rates and concentrations, because of the ion concentration change during the CV measurements is about one tenth of the total ion concentration. The micro-reactor has a potential difference between the anodic and cathodic peaks of about 0.1 V, suggesting that the distance between two Au electrodes is sufficient to apply macro-cell consideration for the electrochemistry of the cell. The peaks increase with increasing scanning rate, however, the potential of the peak current is almost completely independent of scanning rate.

Figure 7 shows changes in anodic peak current with concentration of the [$K_3Fe(CN)_6$ + $K_4Fe(CN)_6$], here the peak current increases with concentration at different scanning rates. At the same concentration, a faster scanning rate results in a higher peak current. These results suggest that the micro-reactor can be used to analyze small volumes and low environmental concentrations of ions and in other applications.

3.3 Electrochemical performance with flowing solution

Figure 8 shows the CV obtained by the micro-reactor at a flow rate of 1.0 µl/s in [$K_3Fe(CN)_6$ + $K_4Fe(CN)_6$]. The concentration of reactants is 20 mol/m^3 (ratio 1:1). There are no anodic and cathodic peak currents, but anodic and cathodic limiting

currents appear at every potential scanning rate. These limiting currents increase slightly with increasing potential scanning rate.

Figure 9 is the CV obtained by the micro-reactor at different flow rates. The concentration of reactants is 20 mol/m^3 and the potential scan rate is 50 mV/s, here, the limiting currents depend on the solution flow rate.

Figure 10 shows changes in anodic limiting currents with potential scanning rate at different solution flow rates. The concentration of reactants is 20 mol/m^3. The anodic peak current increases slightly with increasing potential scanning rate at each solution flow rate and it also shows a clear dependence on the solution flow rate. This means that the anodic reaction is controlled by the mass transport.

4. Discussion

4.1 Anodic peak at static conditions

It is well known that the anodic peak current, I_{ap} in the CV of a reversible reaction is explained as follows [28],

$$I_{ap} = 0.4463nFAc\left(\frac{nF}{RT}\right)^{\frac{1}{2}} D^{\frac{1}{2}} \nu^{\frac{1}{2}} \quad (1)$$

where F is the Faraday constant, R is the gas constant, A is the area of anode, T is the temperature, n is the electrons per molecule reaction, and D and c are the diffusion constant and the concentration of the ions. This equation shows that the anodic peak current is proportional to the square root of the potential scanning rate.

Figure 11 shows changes in the anodic peak current with the square root of the scan rate

of the potential at different concentration of the reactants. At both concentrations, the anodic peak current increases linearly with the square root of the potential scanning rate. Because of the geometry of the micro-cell and channel, it is not clear that all of the Au coated area functioned as electrode. With equation (1) and the diffusion constant of ferrous ions, it is possible to estimate the effective electrode area of the reactor. The diffusion constant of ferrous ions in the KCl solution is 0.66 x 10^{-5} to 0.62 x 10^{-5} cm^2/s [29], giving an estimated electrode area of about 1.7 mm^2. This value is slightly less than half of the 4 mm^2 Au coated area. This low effective electrode area may be due to the geometry or shape of the electrode. The cell shape is not ideal and shape must be changed to improve the accuracy of the concentration analysis.

4.2 Limiting current at flow conditions

The electrode arrangement here is different from channel flow electrode systems, however, it may be possible to apply ideas for channel flow electrodes to the system here to analyze the relationship between the limiting current and solution flow rate. In the case of the channel electrode system, the limiting current, I_L and solution flow rate, v, in the channel for laminar solution flow conditions is expressed as follows [30, 31]

$$I_L = 1.165nFCw\left(\frac{vD^2x^2}{b}\right)^{\frac{1}{3}} \quad (2)$$

where, F is the Faraday constant, n is the electrons per molecule reaction, D is the diffusion constant of the ions, v is the mean flow rate of the solution, C is the concentration of the reactant in the bulk solution, w is the width of the electrode, b is the

half depth of the micro-channel, and x is length of the electrode. This equation shows that when the solution flow is laminar, the limiting current is proportional to the cubic root of the solution flow rate.

It is difficult to estimate flow rates in the micro-cell and all the flow experiments were performed with the same reactor, therefore, the volume flow rate is used as an alternative to the flow rate. Figure 12 shows changes in anodic limiting current with cubic root of solution flow rate at different concentration of the reactants and a scanning rate of 5 mV/s. At both concentrations, the anodic limiting current increases linearly with increasing cubic root of solution flow rate. This suggests that even at the fastest solution flow rate, 1 μl/s, the flow mode is still laminar and that it is possible to measure the concentration and diffusion constants of a species.

5. Conclusions

A combination of anodizing, laser irradiation, and electroplating was applied to fabricate a three electrode type micro-electrochemical reactor and the performance of measurements of electrochemical reactions with a reactor of these components was examined. The following conclusions may be drawn.

1) It is possible to fabricate the elements of a three electrode type electrochemical micro-reactor on anodized aluminum by a combination of anodizing, laser irradiation, and electroplating.

2) It is also possible to measure the cyclic voltammogram which depends on the concentration of reactants and potential scanning rate by the fabricated micro-reactor

with both static and flowing reactant solutions.

3) Peak currents are obtained at static conditions and the anodic peak current increases with the square root of the potential sweep rate.

4)There is a limiting current of the reactions at a solution flow condition and the anodic limiting current is proportional to the cubic root of the solution flow rate.

Acknowledgement

The authors are indebted for financial support in the form of a Grant-in-Aid for Exploratory Research from the Japan Society for the Promotion of Science.

References

[1] D. J. Harrison, A. Manz, Z. Fan, H. Ludi and H. M. Widmer, Anal. Chem., 64 (1992) 1926.

[2] A. Daridon, M. Sequeira, G. Thomas, H. Diarac, J. Krog, P. Gravesen, J. Lichtenberg, D. Diamond, E. Verpoorte and N. Roooij, Sensors and Actuator, B 76 (2001) 235.

[3] J. Ball, D. Scott, J. Lumpp, S. Daunert, J. Wang and L. Bachas, Anal. Chem., 72 (2000) 197.

[4] T. Kamidate, T. Kaide, H. Tani, E. Makino and T. Shibata, Anal. Sci., 17 (2001) 951.

[5] T. Kamidate, T. Kaide, H. Tani, E. Makino and T. Shibata, Luminescence, 16 (2001) 337.

[6] K. Ueno, H. Kim, H. Misawa and N. Kitamura, Anal Chem., 75 (2003) 2086.

[7] K. Ueno, H. Kim and N. Kitamura, Anal. Sci., 19 (2003) 391.

[8] K. Ueno and N. Kitamura, Analyst, 128 (2003) 1401.

[9] N. Kitamura, Electrochemistry,75 (2007) 70.

[10] L. Baars-Hibbe, P. Sichler, C. Schrader, C. Geßner, K. -H. Gericke and S. Büttgenbach, Surface and Coatings Technology, 174-175 (2003) 519.

[11] P. Watts, S. J. Haswell and E. Pombo-Villa, Chem. Eng. J., 101 (2004) 237.

[12] O. Demoulin, M. Navez, F. Gracia, E. E. Wolf and P. Ruiz, Catalysis Today, 91-92, (2004) 85.

[13] R. Schenk, V. Hessel, C. Hofmann, J. Kiss, H. Löwe and A. Ziogas**,** Chem. Eng. J., 101, Issues 1-3 (2004) 421.

[14] J. Yoshida and S. Sugai, Electrochemistry,75 (2007) 58.

[15] D. Horii and M. Atobe, Electrochemistry,75 (2007) 62

[16] Y. Matsushita, Electrochemistry,75 (2007) 66.

[17] M. Sakairi, J. Wakabasyshi, H. Takahashi, Y. Abe and N. Katayama, J. Surf. JPN., 49 (1998) 1227.

[18] S. Z. Chu, M. Sakairi, H. Takahashi, and Z. X. Qiu, J. Electrochem. Soc., 146 (1999) 546

[19] S. Z. Chu, M. Sakairi, and H. Takahashi, J. Electrochme. Soc., 147 (2000) 1423.

[20] S. Z. Chu, M. Sakairi, and H. Takahashi, K. Shimamura and Y. Abe, J. Electrochme. Soc., 147 (2000) 2181.

[21] M. Sakairi, Z. Kato, S. Z. Chu, H. Takahashi, Y. Abe, and N. Katayama,

Electrochemistry, 71 (2003) 920.

[22] T. Kikuchi, M. Sakairi, H. Takahashi, Y. Abe, and N. Katayama, Surface and coatings technology, 169-170 (2003) 199.

[23] T. Kikuchi, M. Sakairi and H. Takahashi, J. Electrochem. Soc. 150 (2003) C567.

[24] T. Kikuchi, M. Sakairi, H. Takahashi, Y. Abe, and N. Katayama, J. Electrochem. Soc., 148 (2001) C740.

[25] Y. Akiyama, T. Kikuchi, M. Ueda, M. Iida, M. Sakairi and H. Takahashi, Electrochim. Acta, 51 (2006) 4834.

[26] H. Jha, T. Kikuchi, M. Sakairi and H. Takahashi, submitted to Electrochim. Acta.

[27] M. Sakairi, M. Yamada and H. Takahashi, Electroche. Soc. Proc., 19 (2004), 359.

[28] A. J. Bard and L. R. Faulkner, "Electrochemical methods - Fundamentals and applications", John Wiely & Sons, Inc., New York, (1980) 218.

[29] R. N. Adams, "Electrochemistry at solid electrodes", Marcel Dekker Inc., New York (1962) 219.

[30] V. G. Leivich, Physicochemical Hydrodynamics, Prinic-Hall, Englewood Cliffs, N. J., (1962) 112.

[31] M. Saeki, A. Nishikata and T. Tsuru, Denki kagaku (present Electrochemistry), 64 (1996) 891.

Captions

Fig. 1 Schematic drawing of the fabrication process of the plates.

Fig. 2 Schematic outline of the cross section of the electrochemical micro-reactor and the electrochemical measurement unit.

Fig. 3 Appearance of the fabricated Plate I and Plate II.

Fig. 4 CSLM contrast images of fabricated parts of the micro-reactor.

Fig. 5 a)schematic illustration and b) top view of the assembly with the micro-reactor.

Fig. 6 CV of the micro-reactor at static (reagents not flowing) conditions in [$K_3Fe(CN)_6$ + $K_4Fe(CN)_6$] at reagent concentrations of 200 mol/m^3 and 20 mol/m^3 in a 1:1 ratio at different scanning rates.

Fig. 7 Changes in the anodic peak current with concentration of $K_3Fe(CN)_6$ / $K_4Fe(CN)_6$ at different scanning rates.

Fig. 8 CV at different scanning rates obtained by the micro-reactor at a flow rate of 1.0 µl/s in [$K_3Fe(CN)_6$ + $K_4Fe(CN)_6$]. The concentration of reactants is 20 mol/m^3.

Fig. 9 CV obtained by the micro-reactor at different flow rates. The concentration of reactants is 20 mol/m^3 and the potential scanning rate is 50 mV/s.

Fig. 10 Changes in the anodic limiting current with the potential scanning rate at different solution flow rates. The concentration of reactants is 20 mol/m^3.

Fig. 11Changes in the anodic peak current with the square root of potential scanning rate at different concentration of the reactants.

Fig. 12 Changes in the anodic limiting current with the cubic root of the solution flow rate at different concentration of the reactants and a scanning rate of 5 mV/s.

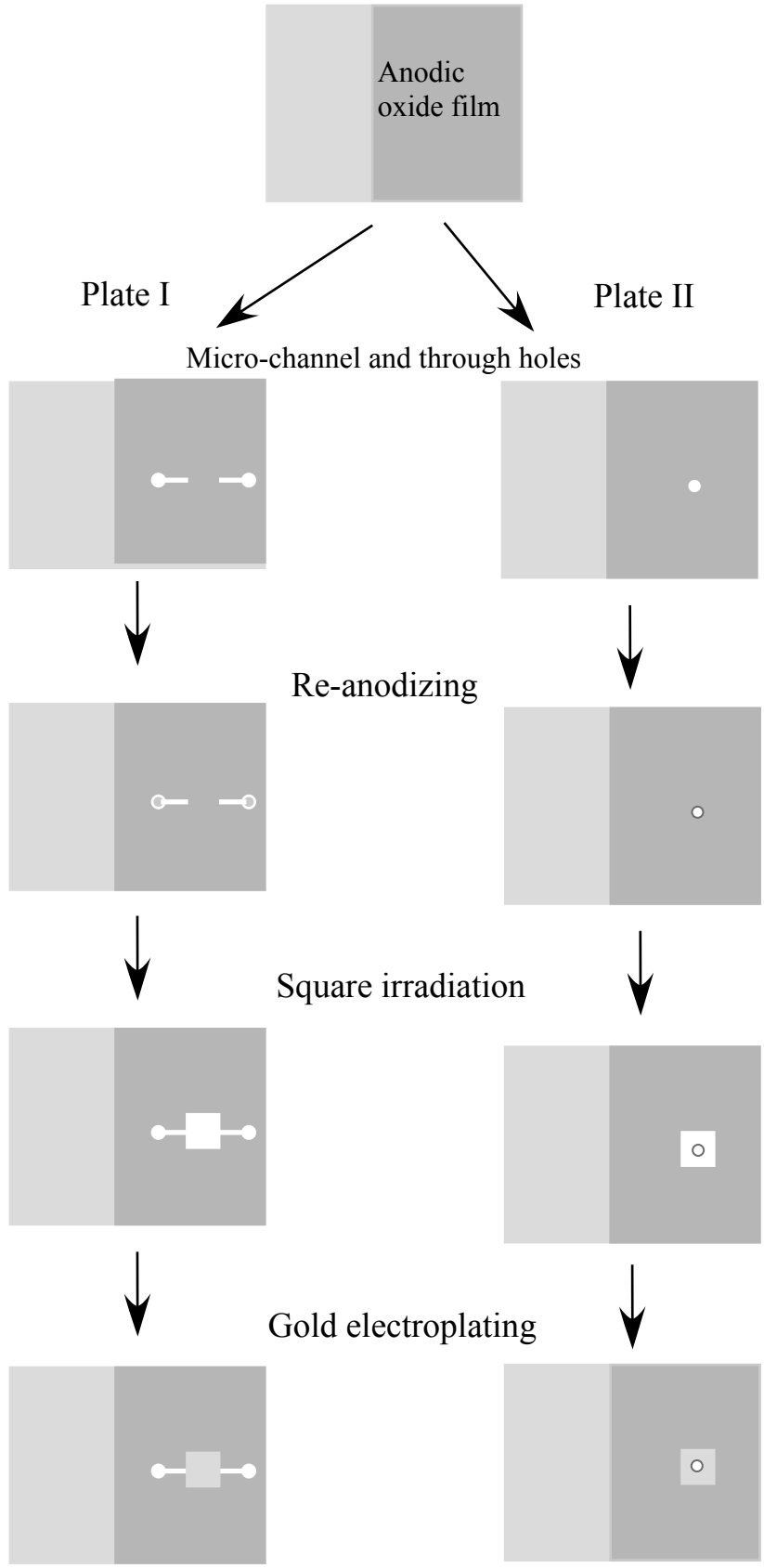

Fig. 1

Sakairi et al.

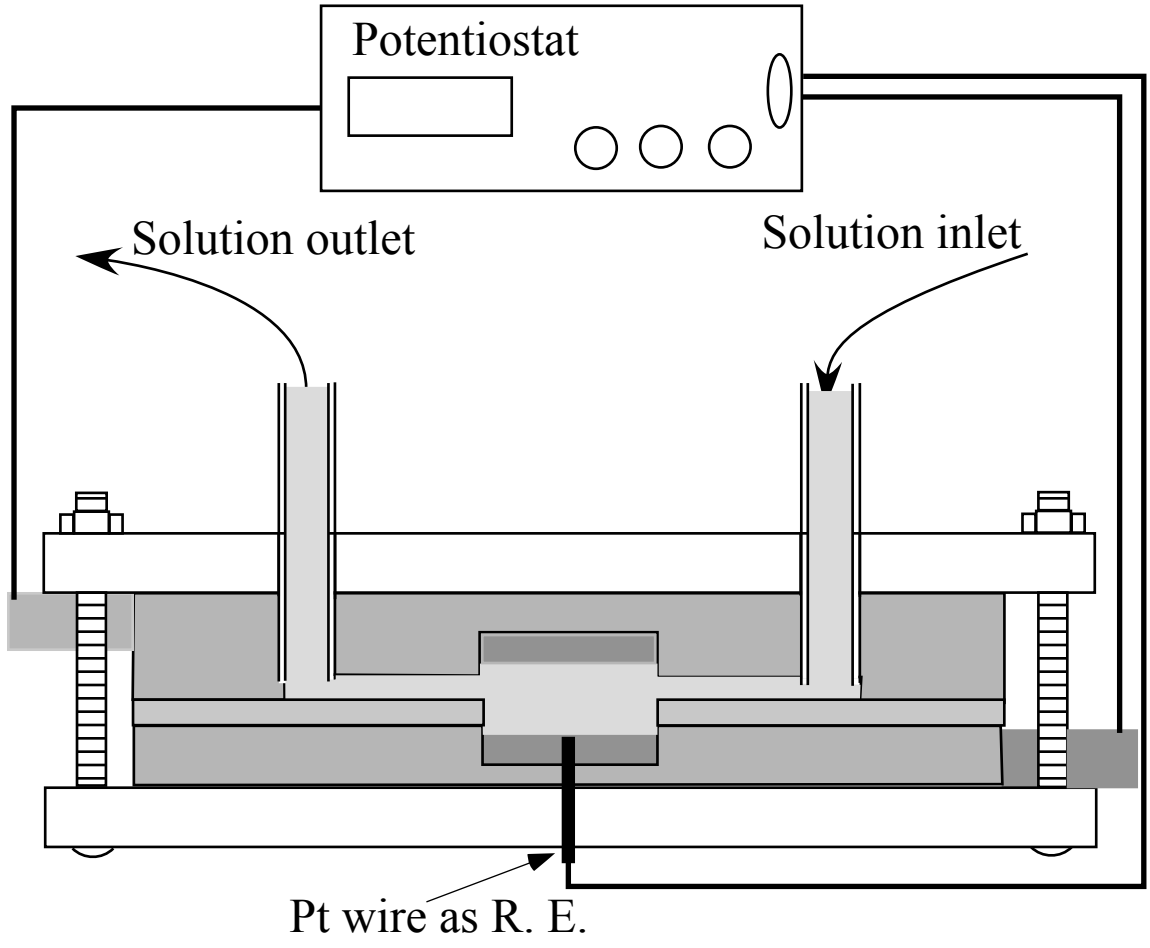

Fig. 2

Sakairi et al.

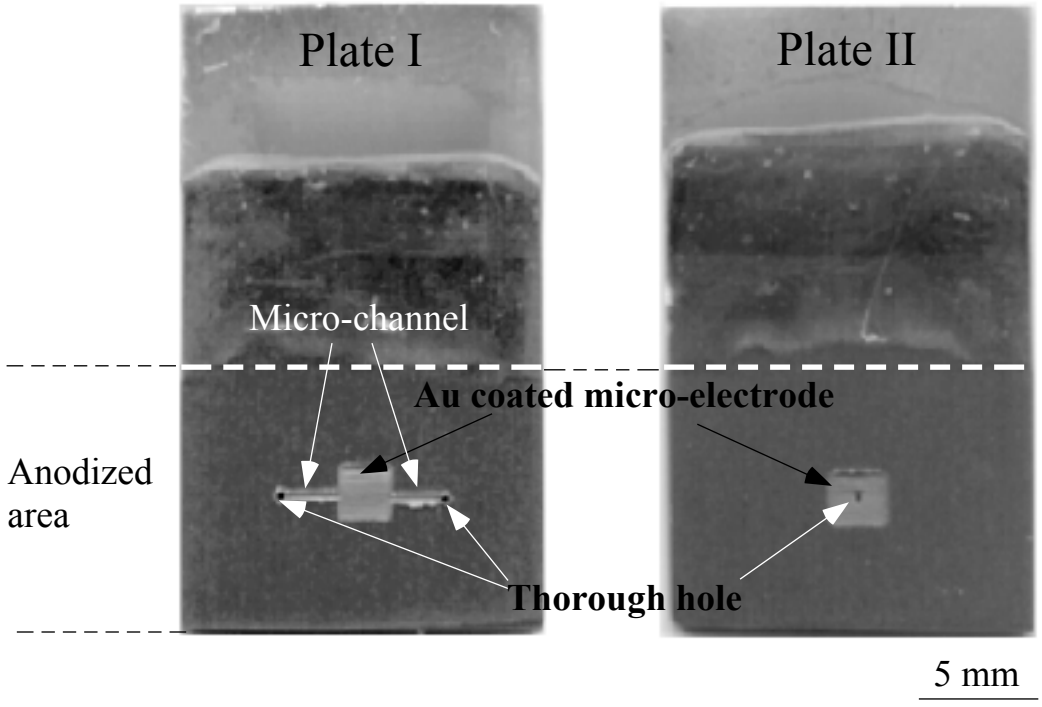

Fig. 3

Sakairi et al.

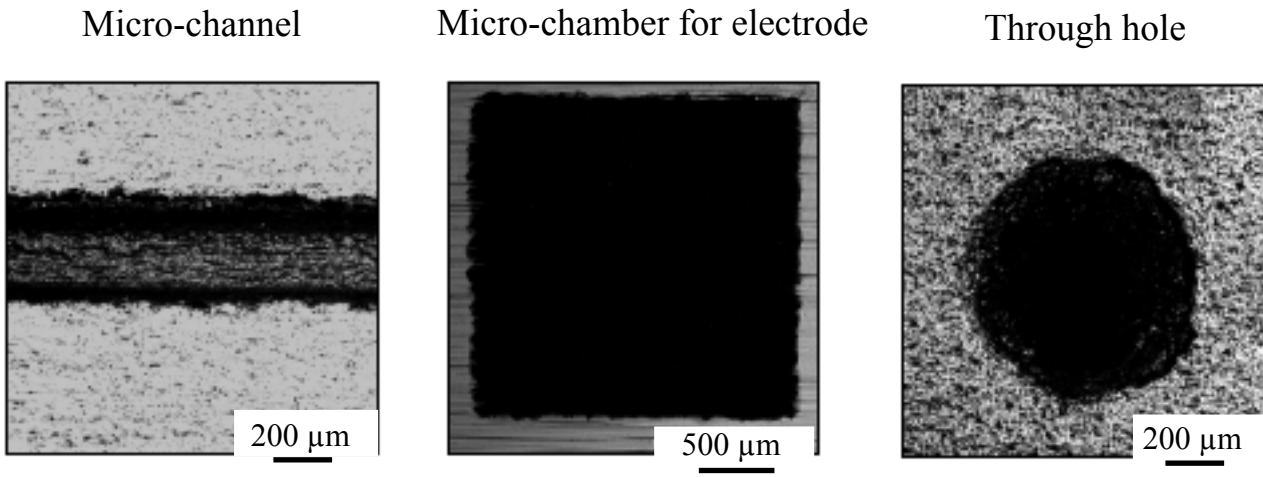

Fig. 4

Sakairi et al.

a)

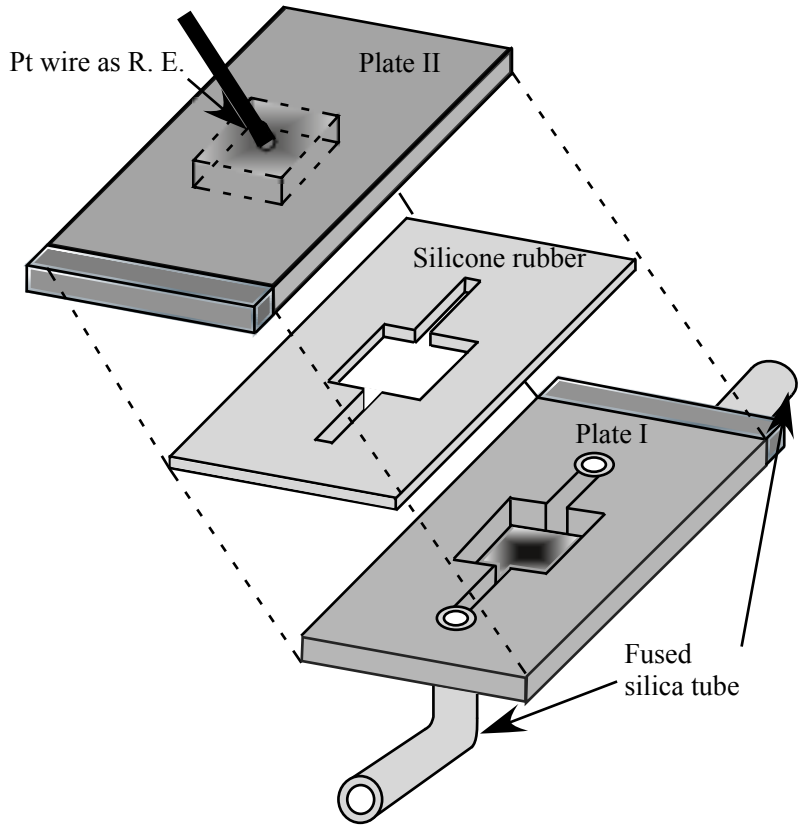

b)

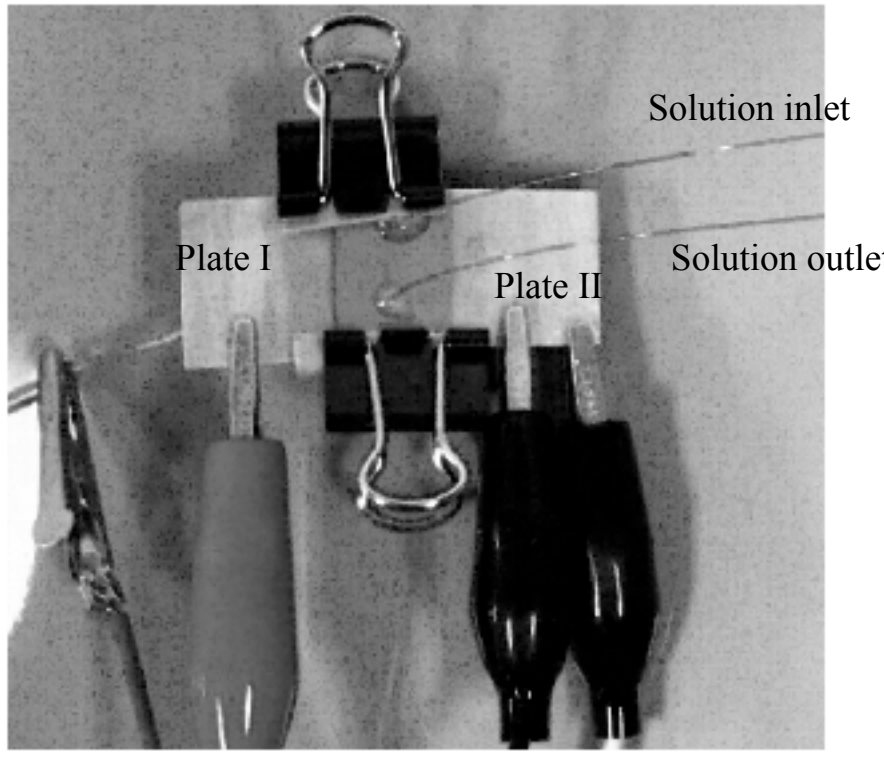

Fig. 5

Sakairi et al.

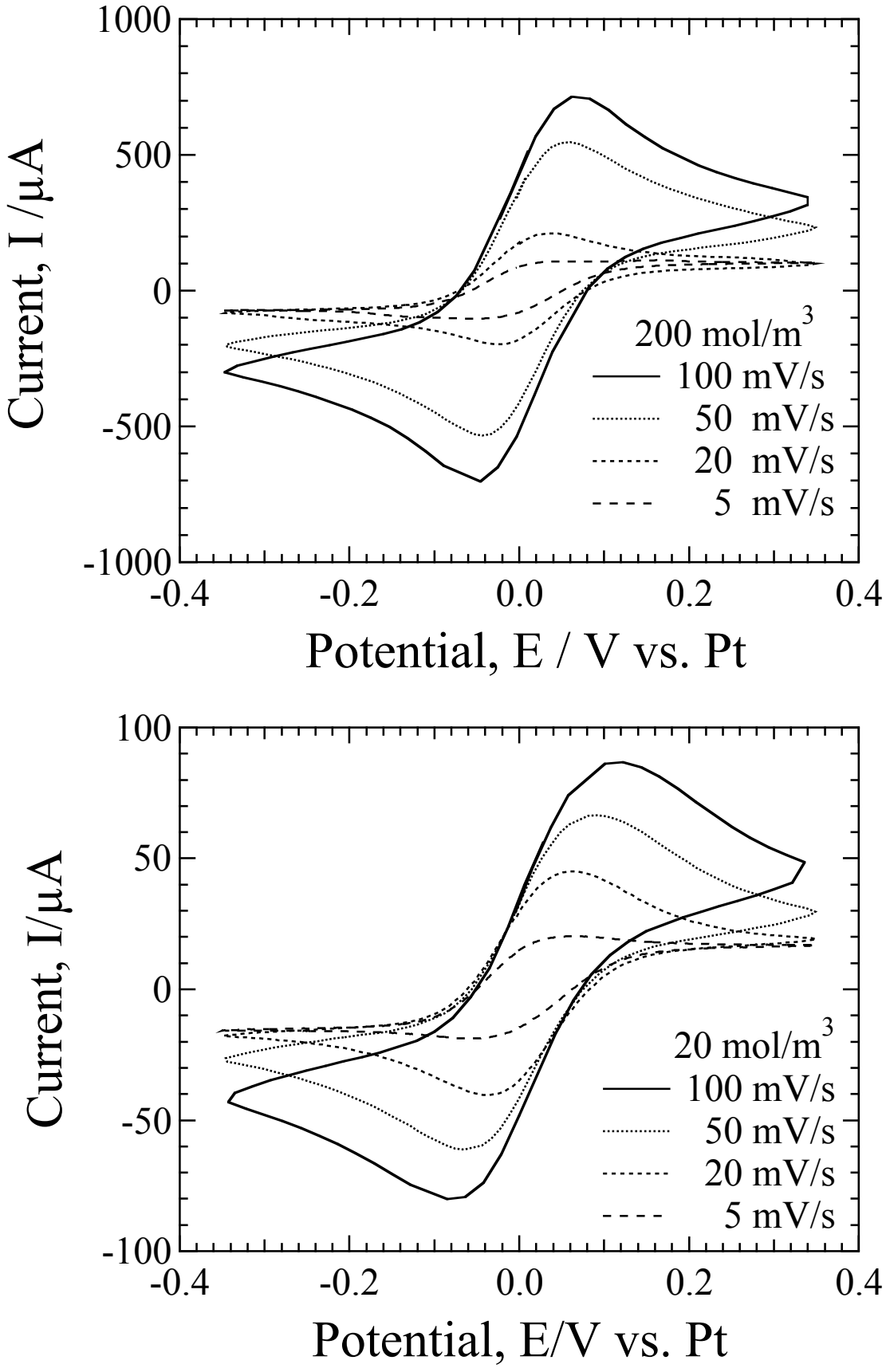

Fig. 6

Sakairi et al.

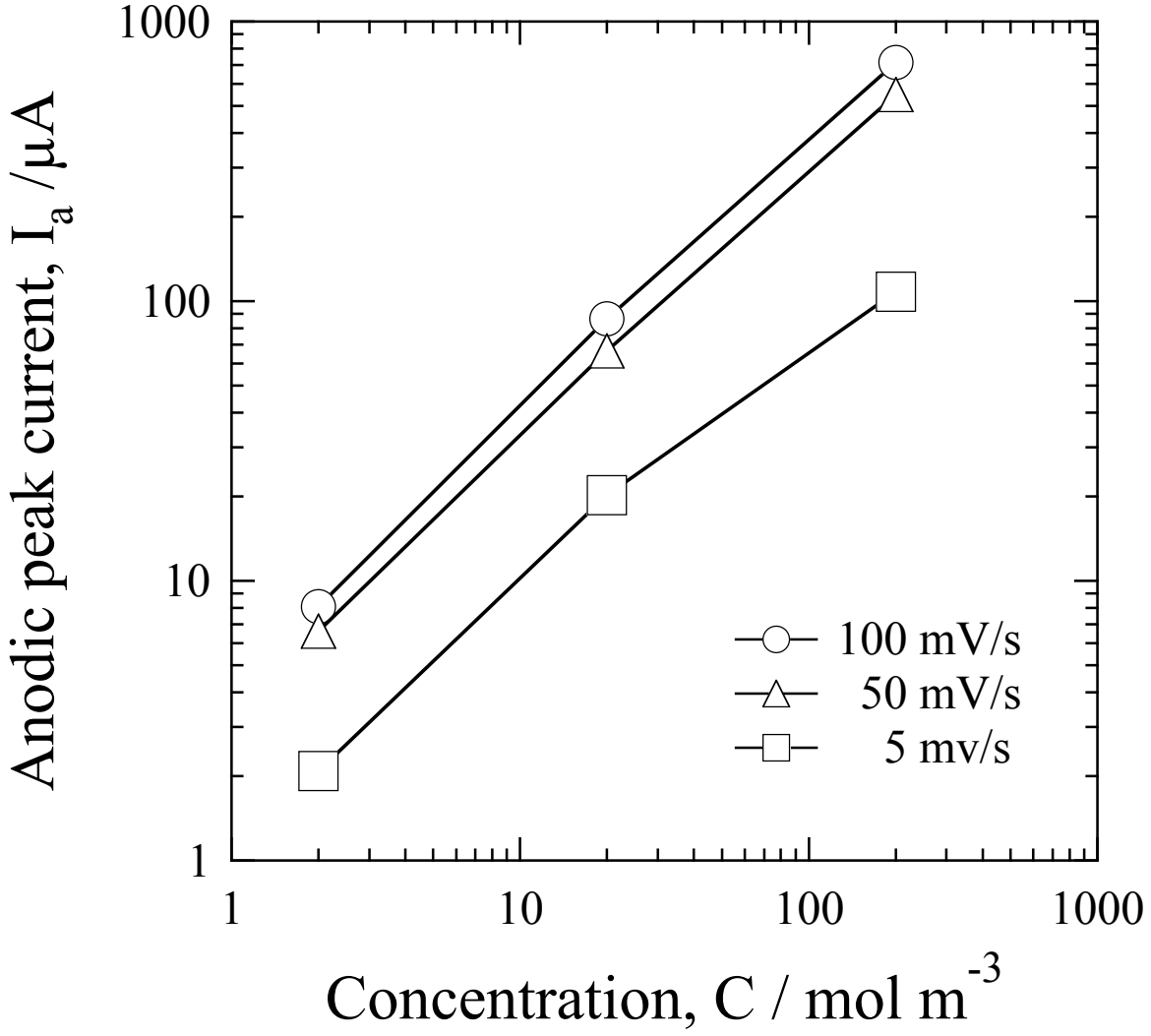

Fig. 7

Sakairi et al.

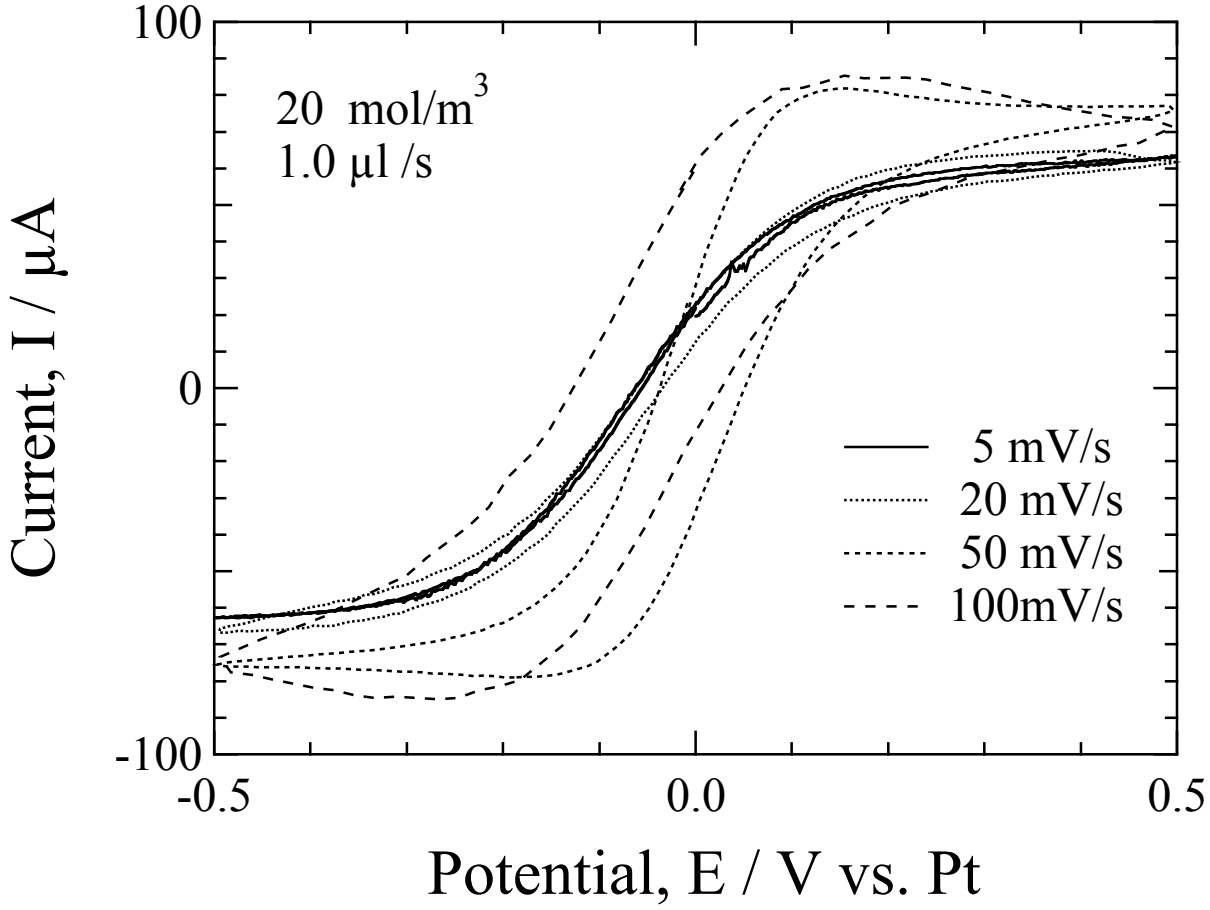

Fig. 8

Sakairi et al.

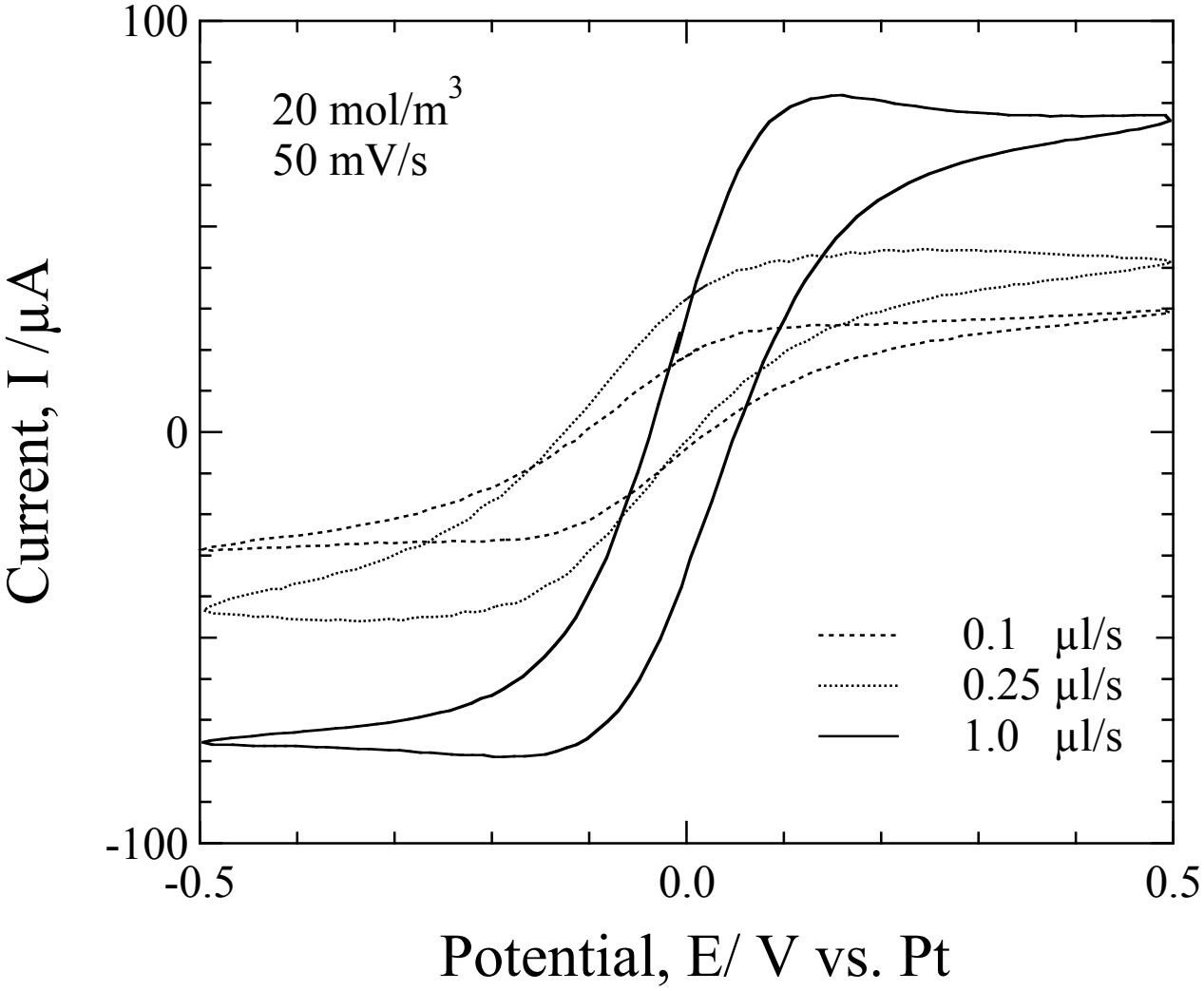

FIg. 9

Sakairi et al.

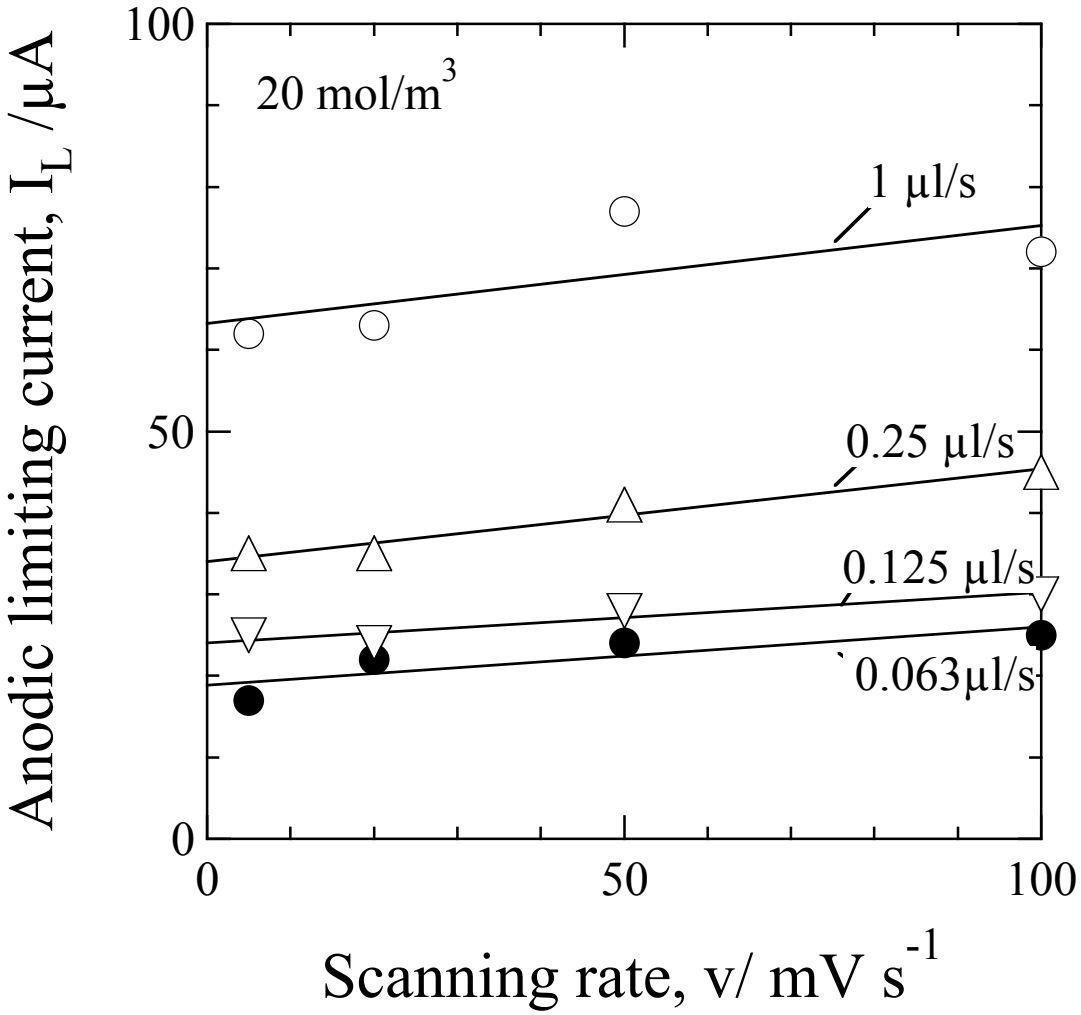

Fig.10

Sakairi et al.

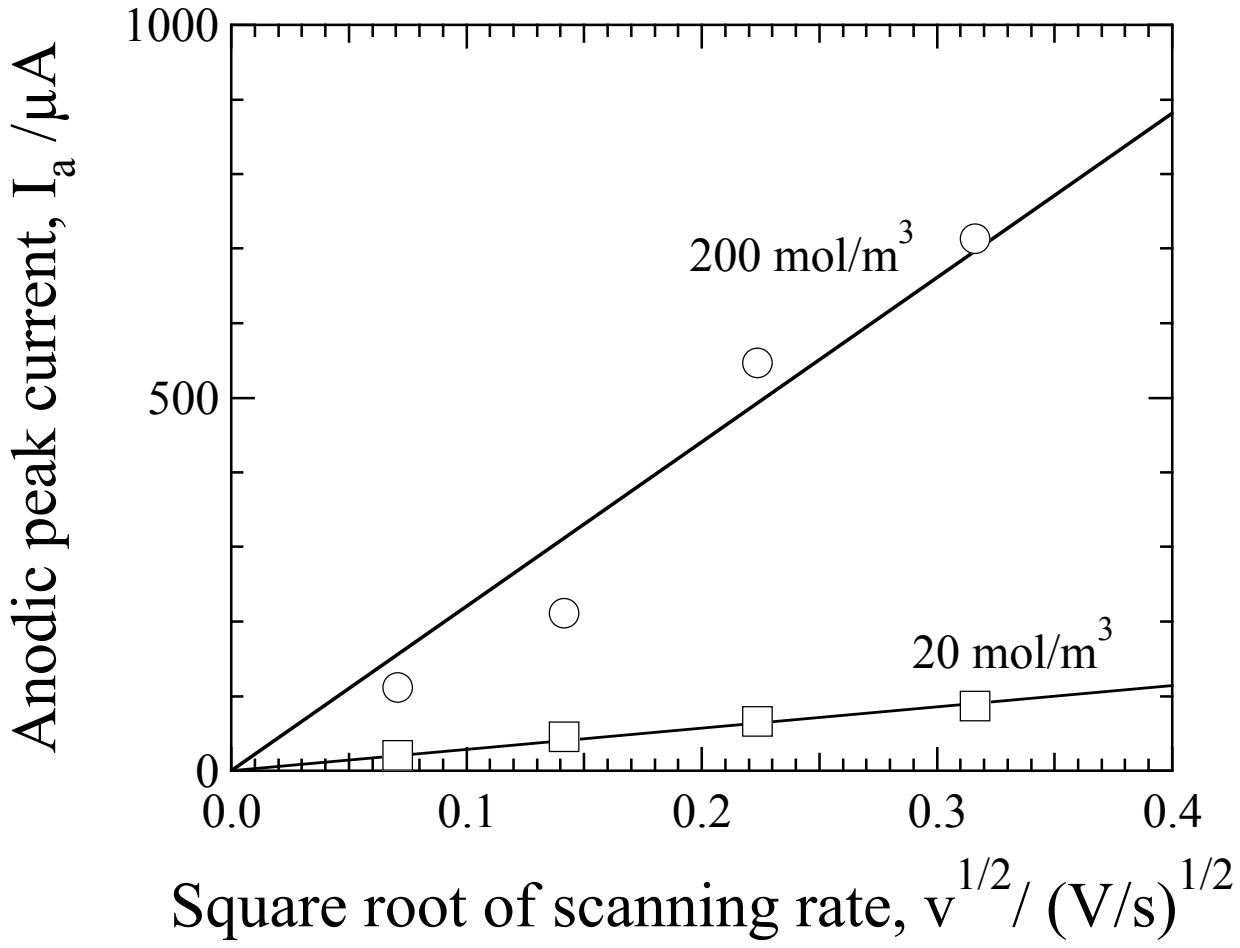

Fig. 11

Sakairi et al.

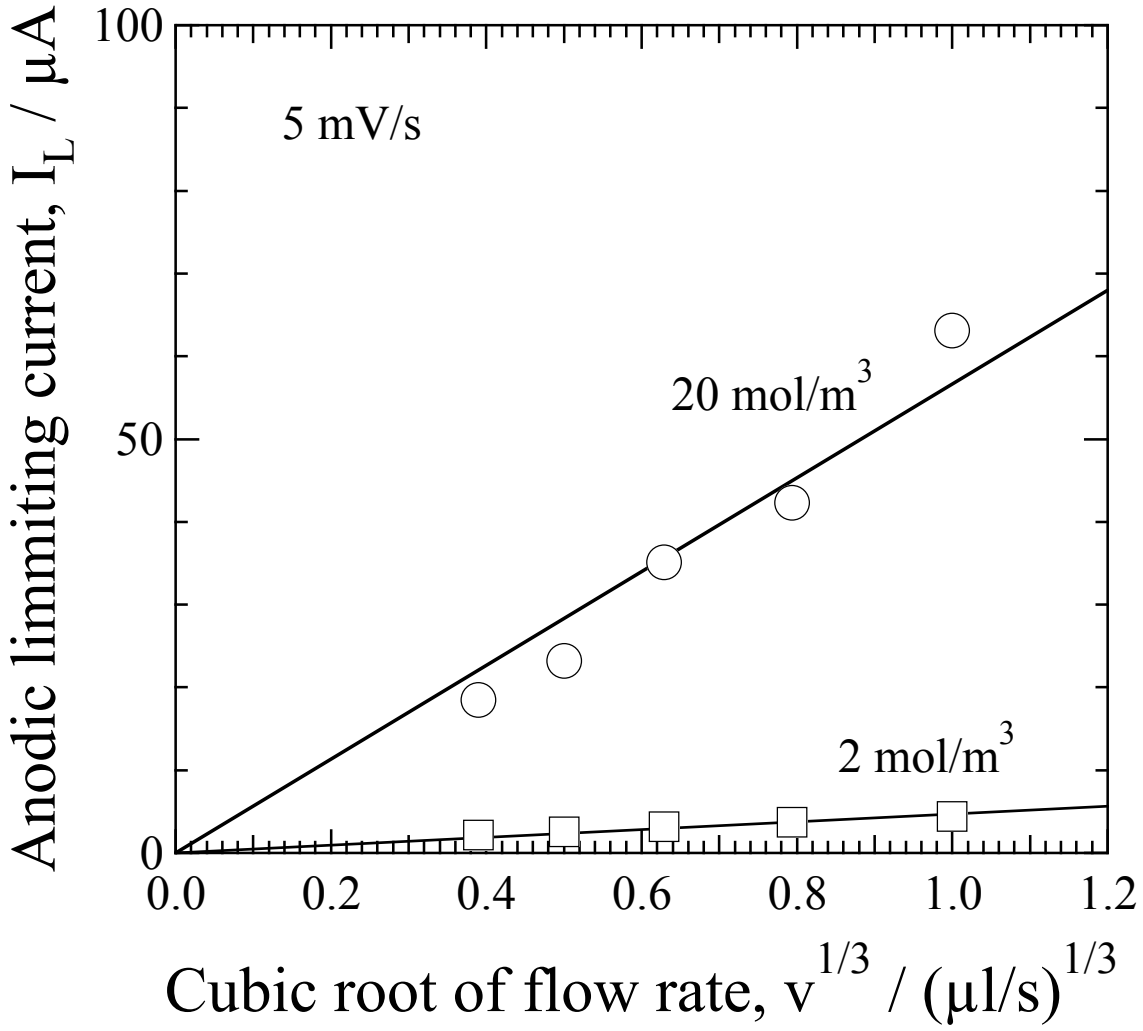

Fig. 12 Sakairi et al.